Polymorphism and π Stacking Affect Thermal

Expansion Behavior in Halogen-Bonded Cocrystals

Based on 1,4-Diiodoperchlorobenzene

Gary C. George III,^{a,b} Mahshad Karimi,^b Navkiran Juneja,^b Daniel K. Unruh,^b Ryan H. Groeneman*,^c and Kristin M. Hutchins*,^{a,b,d}

^aDepartment of Chemistry, University of Missouri, Columbia, Missouri, 65211, United States. Email: kristin.hutchins@missouri.edu.

^bDepartment of Chemistry and Biochemistry, Texas Tech University, Lubbock, Texas, 79409, United States.

^cDepartment of Natural Sciences and Mathematics, Webster University, St. Louis, Missouri, 63119, United States. Email: ryangroeneman19@webster.edu

^dMU Materials Science & Engineering Institute, University of Missouri, Columbia, Missouri, 65211, United States.

KEYWORDS

Cocrystal, Thermal Expansion, Halogen Bonding, Polymorphs

ABSTRACT

The thermal expansion behavior of a series of halogen-bonded cocrystals containing 1,4-diiodoperchlorobenzene as the donor is described. Two of the solids are polymorphs and contain 4-stilbazole as the acceptor, while the third solid contains 4-(phenylethynyl)pyridine as the acceptor and this solid is isostructural with one of the polymorphs. All solids are sustained by I···N halogen bonds, and the least thermal expansion occurs along this direction in all solids. The polymorphs exhibit significant differences in π stacking, and we show that electronically similar face-to-face stacked rings undergo more expansion when compared to electronically different stacked rings. Moreover, in the two polymorphs, the directions of moderate and most expansion are reversed, demonstrating how cocrystal polymorphism can affect material properties.

1. INTRODUCTION

Controlling the three dimensional self-assembly of organic molecules into a solid-state structure remains challenging for crystal engineers and materials scientists. The extended solid-state structure, as well as the intermolecular forces sustaining the solid have a direct influence on the properties of the material. $^{1-3}$ Π -stacking interactions, 4,5 for example, play a role in protein folding and binding of small molecules, 6 affect conductivity in organic semiconductors, 7,8 and can be used to drive molecular recognition. 9,10 One property affected by solid-state structure and intermolecular forces is thermal expansion (TE); the response of a material to temperature change. Stronger intermolecular interactions, such as halogen and hydrogen bonds, are typically less affected by temperature than weaker interactions, 11 such as π stacking. Several studies have

demonstrated the correlation between intermolecular interaction type and TE and the type of interaction can be used as a way to control TE in solid materials. 12-16 This concept has been referred to as interaction dependence. 17,18

One focus within our research is to understand the role that intermolecular forces, extended solid-state structure, and molecular motion play in the TE properties for both organic and inorganic solids. Specifically, we have reported that motion-capable functional groups such as the azo (N=N) or ethylene (C=C) will yield larger TE tensors along the direction in the solid where this motion happens if the group undergoes solid-state pedal motion. Moreover, the tensors are larger in solids that undergo motion when compared to those containing a rigid group, such as acetylene (C=C), which is not capable of pedal motion. Recently, we reported the roles of molecular pedal motion and ligand stacking on the TE parameters for a series of related silver(I) coordination complexes. In these discrete-based assemblies, ligands π -stacked in an edge-to-face or face-to-face geometry, and polymorphic behavior was also observed. We determined that the combination of pedal motion and an edge-to-face stacking of the aromatic rings resulted in the largest TE within these silver-based solids.

Using this as inspiration, we sought to investigate influences of π stacking differences and motion capability in a system sustained by halogen bonds. Previously, cocrystallization of diiodoperchlorobenzene (C6I2CI4) with 4-stilbazole (SB) has been reported to yield a pair of polymorphic solids.²³ The components within the two polymorphs are held together by the same type of halogen bonds; however, they exhibit differences in π stacking geometries (face-to-face vs. edge-to-face) and extended crystal packing, and TE properties have not been investigated. We selected this known polymorphic system, then, to investigate the influence of molecular pedal motion,²⁴ we also choose 4-(phenylethynyl)pyridine (PAB) as a motion-incapable halogen-

bond-acceptor molecule. We expected that cocrystallization of **PAB** with the same halogen-bond donor ($C_6I_2CI_4$) would yield a solid that was isostructural with one of the two polymorphs featuring **SB**. Here, we describe the solid-state structure of the cocrystal containing $C_6I_2CI_4$ and **PAB**, as well as the TE behavior for the series of related halogen-bonded solids that contain $C_6I_2CI_4$ along with either **SB** or **PAB** as the acceptor (Scheme 1). These unsymmetrical halogen-bond acceptors are either capable of molecular pedal motion (**SB**) or incapable of motion (**PAB**) to investigate if molecular motion occurs and how it might affect the TE parameters. We show that differences in π stacking geometries impacts the direction where expansion occurs in each solid, and less expansion occurs along the direction where aromatic rings are stacked edge-to-face when compared to the direction where rings are stacked face-to-face. Moreover, we show face-to-face stacked aromatic rings that are electronically similar undergo more expansion than face-to-face stacked aromatics which are electronically different.

SCHEME 1. (a) Molecules used in this study. (b) Self-assembly through primary I···N halogen bonds. (c) 1D assembly through I···N halogen bonds and C-H···Cl contacts (shown with SB as an example).

2. EXPERIMENTAL

The compounds C₆I₂Cl₄, SB, and PAB were synthesized using reported or modified methods²⁵⁻²⁷ (see SI). Crystals of (C₆I₂Cl₄)·(PAB) and both forms of (C₆I₂Cl₄)·(SB) were prepared through slow evaporation of a toluene solution. In the cases of the polymorphic cocrystals with SB, the polymorphs crystallized concomitantly (see SI). Each cocrystal was characterized using powder X-ray diffraction (at room temperature) and variable-temperature single-crystal X-ray diffraction. The variable temperature single-crystal X-ray data was collected over a temperature range of 290-190 K in 20 K increments. The TE parameters were calculated using the variable temperature single-crystal X-ray data and the software PASCal²⁸ (Figures S1-S6). Mercury was used to measure intermolecular interaction distances and calculate the root mean square deviation (RMSD) of isostructurality.²⁹ ISOS was also used to calculate unit cell similarity.^{30,31} Powder X-ray diffraction demonstrated bulk purity of (C₆I₂Cl₄)·(PAB) and concomitant polymorphism for (C₆I₂Cl₄)·(SB) (Figures S7-S8). Differential scanning calorimetry (DSC) was used to characterize the thermal behavior of the concomitant polymorphs (Figure S11-S12). DSC was performed on the mixture by heating the sample from 25 °C to 200 °C, followed by cooling the sample back to 25 °C. The experiment was conducted using a heating/cooling rate of either 5 °C/min or 2 °C/min.

3. RESULTS AND DISCUSSION

Crystal Structures of the Solids. The components of (C₆I₂Cl₄)·(PAB) crystallized in the triclinic space group *P-1* (Figure 1). The asymmetric unit contains one molecule of PAB and one half of a molecule of C₆Cl₄I₂. One molecule of C₆Cl₄I₂ interacts with two molecules of PAB via I···N halogen bonds to form the targeted assembly. Each molecule of C₆Cl₄I₂ also engages in

two C-H···Cl contacts with the hydrogen atoms in the *para* position of the benzene ring of **PAB** to form a one-dimensional (1D) chain. While the pyridine and benzene ring of **PAB** lie nearly coplanar, the halogenated benzene ring of **C6I2Cl4** is rotated from the plane of the pyridine ring by 70° at 290 K, which supports formation of the 1D chains. Within the 1D chain, **PAB** molecules are stacked in an antiparallel arrangement with the aromatic rings lying face-to-face and separated by ca. 4 Å. Neighboring chains engage in slightly offset and weak $\pi \cdots \pi$ stacking interactions with a separation of 3.846 Å at 290 K. The $\pi \cdots \pi$ separations are both outside of the sum of the van der Waals radii. The two remaining chlorine atoms on **C6I2Cl4** engage in Cl··· π (pyridine) interactions with pyridine rings above and below the 1D chain. The neighboring stacks interact in the third dimension through weak C-H····C-H and C-H····Cl contacts. Along this direction, the **PAB** molecules lie perpendicular to the **C6I2Cl4** molecules (Figure S10a).

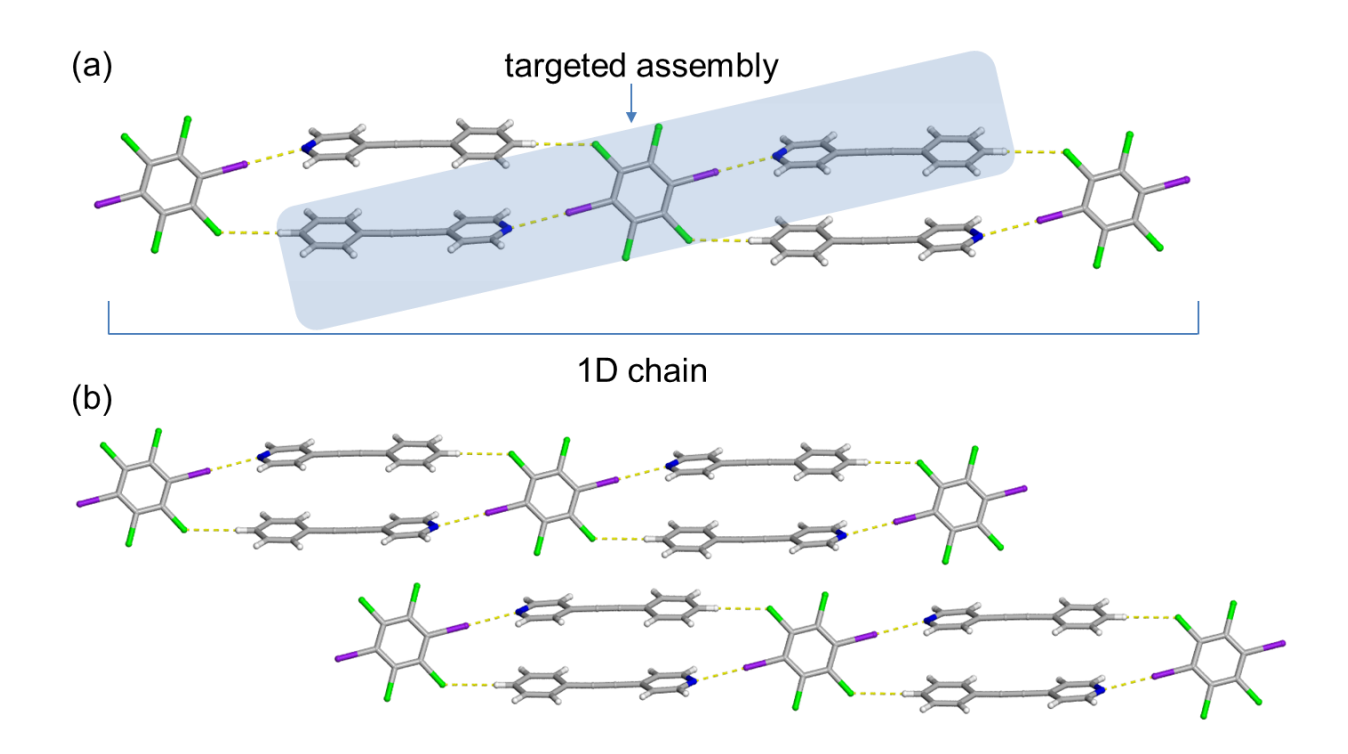


FIGURE 1. X-ray crystal structures of (C₆I₂Cl₄)·(PAB) highlighting (a) targeted assembly through I···N halogen bonds (blue box) and 1D chains through C-H···Cl contacts and (b)

extended packing. I···N halogen bonds and C-H···Cl contacts are shown with yellow dashed lines.

The components of (C612Cl4)·(SB) crystallize as two polymorphs, namely Form I and II, as previously described.²³ Form I lies in the triclinic space group P-I, and the cocrystal described above featuring PAB is isostructural with the Form I polymorph (Figure 2a). Using Mercury, the two structures have an RMSD of 0.24.²⁹ Using ISOS, the two structures had a cell similarity of 0.032, wherein identical cells would have a value of zero.^{30,31} In Form I, the halogenated ring of C6I2Cl4 is rotated from the planarity of the pyridine ring of SB by 75°, and the pyridine and benzene rings of SB lie nearly coplanar at 290 K. The SB molecules in the 1D chains lie antiparallel and separated by 4.107 Å, and between chains, the offset face-to-face π ··· π stacking separation is 3.921 Å at 290 K. At all temperatures studied, the olefin groups within SB are disordered over two positions. The disorder is quite small as the major site occupies 90-97% of the position, depending on the temperature (see refinement details in SI). The SB component within the Form I cocrystal undergoes only a small amount dynamic motion over the 100 K temperature range, as the site occupancies change by 7% between 290-190 K (Table S9).

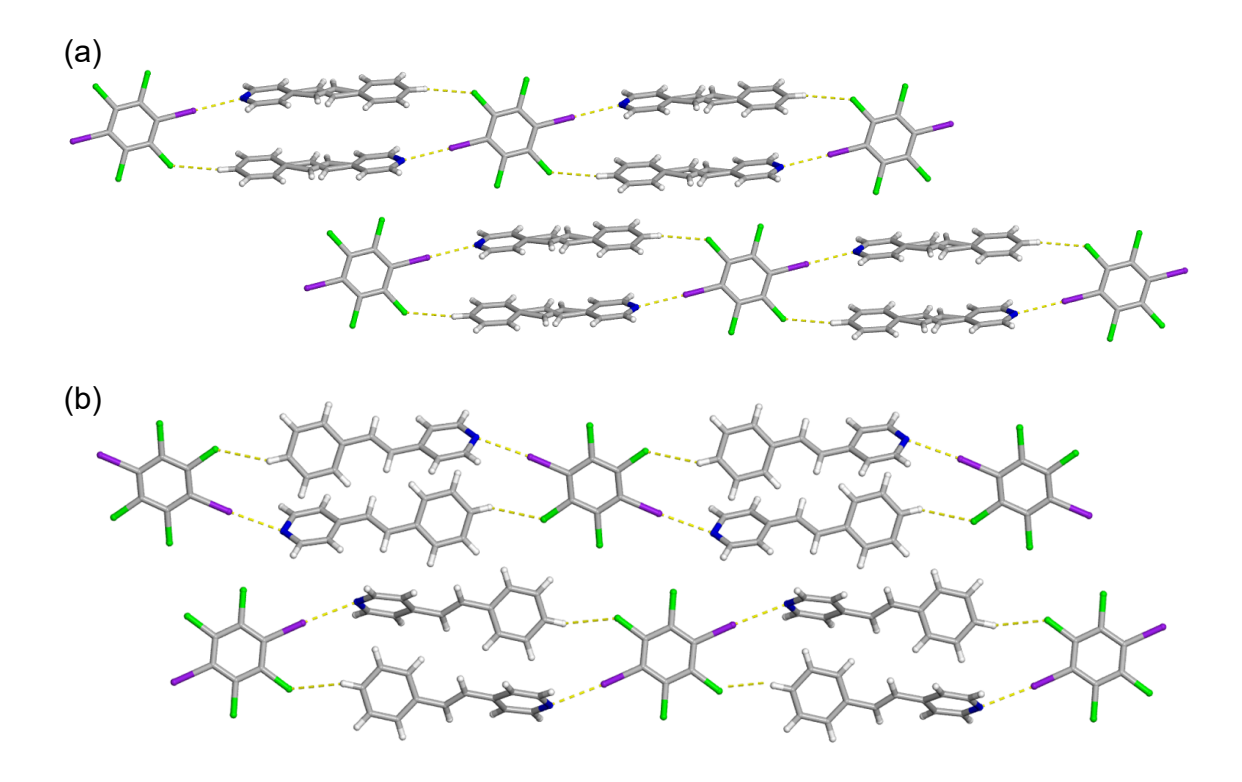


FIGURE 2. X-ray crystal structures of (C₆I₂Cl₄)·(SB): (a) Form I and (b) Form II, highlighting the extended packing (disorder omitted for clarity). I···N halogen bonds and C-H···Cl contacts are shown with yellow dashed lines.

Form II ($C_6I_2CI_4$)·(SB) lies in the monoclinic space group $P2_1/c$.²³ The asymmetric unit contains one molecule of SB and one half of a molecule of $C_6CI_4I_2$, and the components also interact via I···N halogen bonds and C-H···Cl contacts to form the 1D chain. However, the pyridine and benzene rings of SB lie twisted by 56° rather than coplanar. Moreover, the halogenated benzene ring of $C_6I_2CI_4$ lies nearly coplanar with the benzene ring of SB and is rotated from the planarity of the pyridine ring by 68°. Due to the non-planarity of the SB molecules, within the 1D chain, the SB molecules are stacked edge-to-face and separated by 4.530 Å. Moreover, neighboring chains are further engaged in edge-to-face π ··· π stacking with long separations of 5.642 Å (pyridine-pyridine) and 6.245 Å (benzene-benzene) at 290 K (Figure

2b). In the Form I polymorph of (C612C14)·(SB) and (C612C14)·(PAB), neighboring chains are simply translated along this π -stacking direction; however, in the Form II polymorph, the neighboring chains are rotated though a two-fold screw axis. Another difference in Form II arises in the behavior of the halogen-bond donor; the two remaining chlorine atoms on C612C14 engage in a C-H···C1 interaction with a pyridine ring on an adjacent chain instead of C1··· π interactions. The stacks interact in the third dimension through various weak C-H··· π interactions. Along this direction, due to the twisting of the SB molecules, the benzene rings of SB lie parallel to the C612C14 molecules and engage in heterogenous face-to-face π stacks that alternate in an ABA manner (Figure S10b). At all temperatures studied, the SB molecule in Form II is disordered over two positions. The disorder in Form II is more significant as the major site only occupies slightly over half (55-62%) of the position, depending on the temperature (see refinement details in SI). Although the disorder in Form II is more significant than in Form I, the SB component within Form II only undergoes a small amount dynamic motion as the site occupancies also change by 7% over the 100 K temperature range (Table S9).

Characterization of Concomitant Polymorphs. The polymorphs of (C₆I₂Cl₄)·(SB) were isolated concomitantly, as supported by powder X-ray diffraction (Figure S8). Concomitant cocrystallization occurred even when evaporation rates and concentrations were varied. DSC performed on the mixture demonstrated one endothermic signal at 127 °C corresponding to melting, and the signal did exhibit a shoulder at the onset when a heating rate of 5 °C/min was used (Figure S11). Upon cooling from 200 °C to 25 °C, an exothermic signal corresponding to crystallization occurred at 91 °C using a cooling rate of 5 °C/min. The same experiments were conducted using a slower rate of 2 °C/min, and the melting and crystallization signals were within 1 °C of the values from the previous experiment (Figure S12). Prior to the DSC

experiment, powder X-ray diffraction demonstrated the sample contained both polymorphs of (C₆I₂Cl₄)·(SB). Powder X-ray diffraction was conducted for the sample of (C₆I₂Cl₄)·(SB) after completion of the DSC experiment (heating/cooling rate of 2 °C/min) to determine if any change in the sample occurred after the melting and crystallization. The powder X-ray diffraction data shows changes in the sample, and Form II is the dominant phase after melting and crystallization (Figure S9).

Thermal Expansion Behavior. All three solids were stable during the variable temperature single-crystal X-ray diffraction experiment, and no significant structural changes were observed (Figures S4-S6). PASCal²⁸ was used to calculate the principal axes (X₁, X₂, and X₃) and coefficients of TE based on the unit cell parameters from the variable temperature single crystal X-ray data (Table 1). All three cocrystals show zero to slightly positive TE along the principal axis of expansion, X₁. The primary contributions to this direction within the structures include the strong I···N halogen bonds present in each cocrystal, as well as the weaker C-H···Cl interactions that form the 1D chain. The I···N halogen bond lengths shorten by 0.032 Å (1.1% change) for (C₆I₂CI₄)·(PAB), 0.028 Å (1.0% change) for Form I (C₆I₂CI₄)·(SB), and 0.004 Å (0.1% change) for Form II (C₆I₂CI₄)·(SB) upon cooling over the 100 K temperature range studied. The C-H···Cl interactions shorten upon cooling by 0.018 Å (0.5% change) for (C₆I₂CI₄)·(PAB), 0.013 Å (0.3% change) for Form I (C₆I₂CI₄)·(SB), and 0.020 Å (0.5% change) for Form II (C₆I₂CI₄)·(SB) over the same range.

TABLE 1. Linear and volumetric TE coefficients for each cocrystal. Errors are denoted in parentheses and approximate crystallographic axes are denoted in brackets.

Cocrystal	α_{X_1}	(MK^{-1})	α_{X_2}	(MK^{-1})	α_{X_3} (MK ⁻¹)	$\alpha_V(\text{MK}^{-1})$

[axis]	[axis]	[axis]	
-1 (1)	54 (3)	146 (2)	200 (4)
[5 -1 0]	[1 1 -7]	[1 3 0]	
12 (2)	47 (2)	130 (1)	190 (1)
[4 -1 -2]	[4 0 1]	[0 -2 1]	
2 (1) [1 0 -7]	67 (1) [0 -1 0]	112 (1) [2 0 1]	181 (1)
	-1 (1) [5 -1 0] 12 (2) [4 -1 -2] 2 (1)	-1 (1) 54 (3) [5 -1 0] [1 1 -7] 12 (2) 47 (2) [4 -1 -2] [4 0 1] 2 (1) 67 (1)	-1 (1) 54 (3) 146 (2) [5 -1 0] [1 1 -7] [1 3 0] 12 (2) 47 (2) 130 (1) [4 -1 -2] [4 0 1] [0 -2 1] 2 (1) 67 (1) 112 (1)

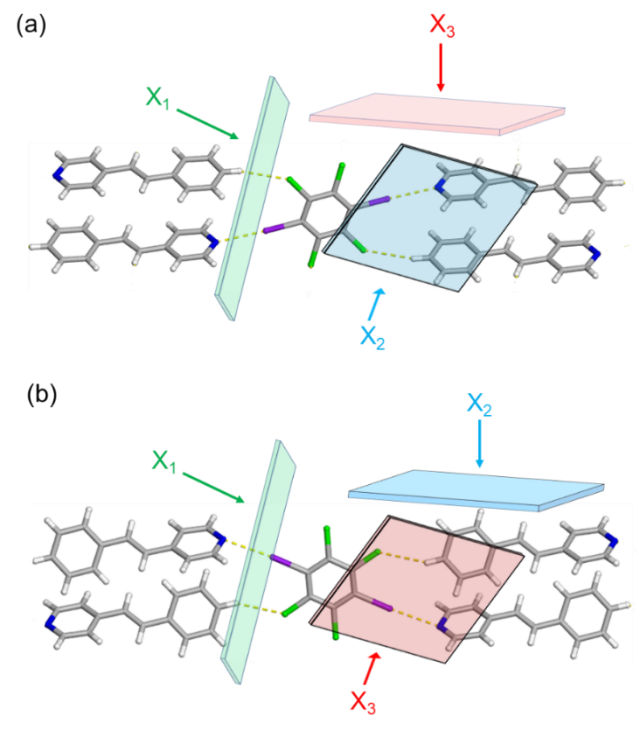


FIGURE 3. X-ray crystal structures of (a) Form I ($C_6I_2Cl_4$)·(SB) and (b) Form II ($C_6I_2Cl_4$)·(SB) highlighting the principal axes of TE, with X_2 and X_3 being reversed in the two structures. The directions of TE for ($C_6I_2Cl_4$)·(PAB) are nearly identical to Form I (part a). The directions of the principal axes of TE are shown by the included planes and arrows, where X_1 is green, X_2 is blue, and X_3 is red.

Although the X_1 axis encompasses a similar direction in the three cocrystals, the directions of X_2 and X_3 differ. Form I (C₆I₂Cl₄)·(SB) and (C₆I₂Cl₄)·(PAB) are isostructural; thus, the X_2 and X₃ directions are similar in the two solids. Both Form I (C₆I₂Cl₄)·(SB) and (C₆I₂Cl₄)·(PAB) exhibit moderate positive TE along X₂, with similar coefficients of 47 and 54 MK⁻¹, respectively. The C-H···C-H and C-H···Cl contacts between stacked chains contribute primarily to the X_2 direction. The X₂ axis also encompasses the direction where molecules are arranged in an offset edge-to-face packing pattern (Figure 4a). On the other hand, TE along X₃ for Form I $(C_6I_2CI_4)\cdot(SB)$ and $(C_6I_2CI_4)\cdot(PAB)$ is dictated primarily by face-to-face $\pi\cdots\pi$ stacking, affording colossal positive TE with coefficients of 130 and 146 MK⁻¹, respectively. These are also the two largest linear TE coefficients in the series of solids. For (C₆I₂Cl₄)·(PAB), the long $\pi \cdots \pi$ interactions decrease upon cooling by 0.045 Å within the chain and 0.058 Å between chains. Form I (C₆I₂Cl₄)·(SB) also exhibits face-to-face π-stacking due to the rings of the SB molecules being coplanar, and the $\pi \cdots \pi$ separations decrease by 0.066 Å within the chain and 0.049 Å between chains upon cooling. The Cl $\cdots\pi$ (pyridine) interactions, which lie along the same direction as the face-to-face π -stacking direction, also decrease by ca. 0.050 Å upon cooling both solids.

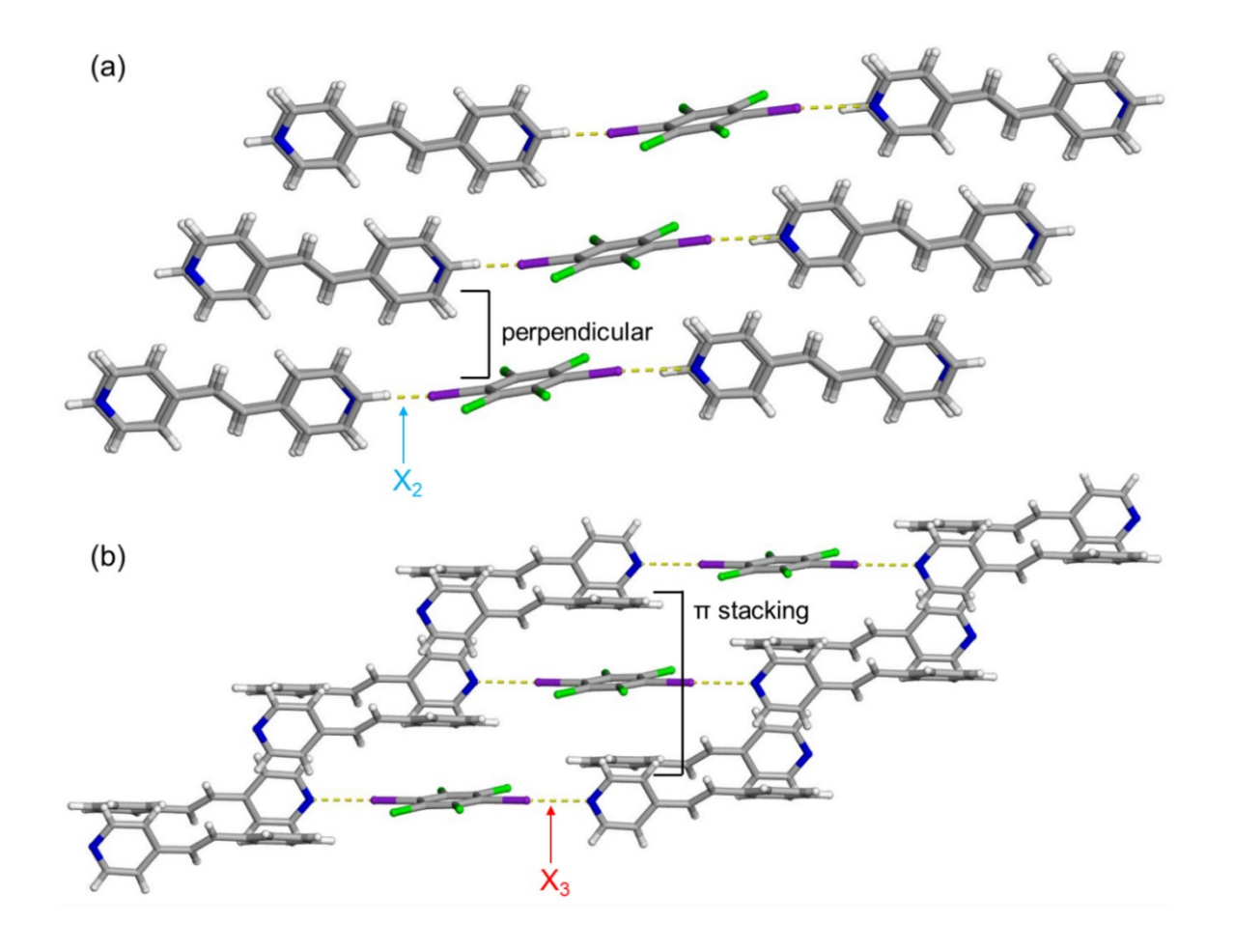


FIGURE 4. X-ray structures at 290 K showing packing in third dimension of (C₆I₂Cl₄)·(SB): (a) Form I and (b) Form II. Disorder is omitted for clarity. The Form I structure is representative of (C₆I₂Cl₄)·(PAB). The relevant axes of TE are also noted. The directions of the principal axes of TE are shown by the included arrows, where X₂ is blue, and X₃ is red.

Interestingly, the directions of X_2 and X_3 in the Form I and II polymorphs of ($C_6I_2Cl_4$)·(SB) are switched (Figure 3). In Form II ($C_6I_2Cl_4$)·(SB), the X_2 direction includes edge-to-face $\pi \cdots \pi$ interactions between stacked 1D chains. Within the 1D chain, the two SB molecules that are arranged edge-to-face undergo a slight increase in distance upon cooling, and the average change upon cooling is ca. -0.010 Å. However, the separations between the stacked 1D chains, which are also arranged edge-to-face, decrease upon cooling by 0.028 Å and 0.052 Å to afford the overall

positive TE. The coefficient of TE along X_2 is 67 MK⁻¹, the largest in the series for the X_2 direction. On the other hand, the X_3 direction encompasses the interactions between stacked chains and the coefficient is the smallest in the series, 112 MK⁻¹. Along the X_3 direction, the C₆I₂Cl₄ molecule engages in face-to-face π stacks with the benzene ring of SB, alternating in an ABA pattern (Figure S10b). These $\pi \cdots \pi$ separations decrease by 0.040 Å upon cooling.

Influence of π Stacking on Thermal Expansion. Saha and coworkers have shown that stronger $\pi\cdots\pi$ stacking interactions exhibit less TE than weaker $\pi\cdots\pi$ stacking interactions.³² Specifically, they showed that a solid containing π -stacked electron deficient and electron rich aromatics exhibited less TE along the stacking axis than a solid containing only π -stacked electron rich rings. The cocrystals (C₆I₂CI₄)·(PAB) and Form I (C₆I₂CI₄)·(SB) exhibit both face-to-face parallel and offset stacked aromatic rings that are electronically similar^{4,33,34} and separated at long distances. Thus, this direction exhibits the most expansion in both solids. For Form II (C₆I₂CI₄)·(SB), the electronically similar rings of SB are stacked edge-to-face, and this direction expands less when compared to the two other cocrystals. Furthermore, along X₃, Form II (C₆I₂CI₄)·(SB) contains face-to-face parallel stacked rings that are electronically different; one is substituted with six halogens while the other is substituted with six hydrogens (Figure 4b). These π interactions, which are electronically different, also undergo less expansion when compared to the other two cocrystals with face-to-face parallel stacked rings that are electronically similar.

4. CONCLUSIONS

Here, we described the TE behavior of a pair of polymorphic solids, wherein the components self-assemble into a 1D chain sustained by the same type of halogen bonds. However, the

polymorphs exhibit significant differences in π stacking, allowing study of the influence face-to-face and edge-to-face stacking has on TE. A novel solid containing a planar molecule was also prepared and determined to be isostructural with one of the polymorphs. The solids sustained by face-to-face parallel and offset stacking of electronically similar aromatics exhibited the largest TE along the stacked direction. The solid containing face-to-face parallel stacked aromatics that are electronically different exhibited less expansion. Cocrystal polymorphs can give differences in properties, and here, although the primary driving force for self-assembly is persistent, the directions of moderate and most expansion are reversed in the two solids. The dependence of TE on intermolecular interaction type has been previously shown for several types of interactions, and here, it is shown for halogen bonds and π stacking. Using specific classes of intermolecular forces to direct self-assembly and corresponding TE will also promote the designability of materials with targeted TE behaviors.

ASSOCIATED CONTENT

Supporting Information. The Supporting Information is available free of charge on the ACS Publications website at DOI:

Experimental details, single-crystal and powder X-ray data, thermal expansion data, and thermal characterization data (PDF).

Accession Codes. CCDC 2308143-2308160 contain the supplementary crystallographic data for this paper. These data can be obtained free of charge via www.ccdc.cam.ac.uk/data request/cif,

or by emailing data request@ccdc.cam.ac.uk, or by contacting The Cambridge Crystallographic

Data Centre, 12, Union Road, Cambridge CB2 1EZ, UK; fax: +44 1223 336033.

AUTHOR INFORMATION

Corresponding Authors

*Email: ryangroeneman19@webster.edu. Tel: +1 314-246-7466

*Email: kristin.hutchins@missouri.edu. Tel: +1 573-882-4598

ORCID: Ryan H. Groeneman: 0000-0002-4602-6287

ORCID: Kristin M. Hutchins: 0000-0001-8792-2830

Notes

The authors declare no competing financial interest.

Author Contributions

The manuscript was written through contributions of all authors. All authors have given approval

to the final version of the manuscript.

ACKNOWLEDGMENT

R. H. G. gratefully acknowledges financial support from Webster University in the form of

various Faculty Research Grants. K. M. H. gratefully acknowledges financial support from the

National Science Foundation DMR-2045506.

REFERENCES

16

- (1) Bedeković, N.; Piteša, T.; Eraković, M.; Stilinović, V.; Cinčić, D. Anticooperativity of Multiple Halogen Bonds and Its Effect on Stoichiometry of Cocrystals of Perfluorinated Iodobenzenes. *Cryst. Growth Des.* **2022**, *22*, 2644-2653.
- (2) Commins, P.; Dippenaar, A. B.; Li, L.; Hara, H.; Haynes, D. A.; Naumov, P. Mechanically compliant single crystals of a stable organic radical. *Chem. Sci.* **2021**, *12*, 6188-6193.
- (3) Eaby, A. C.; Myburgh, D. C.; Kosimov, A.; Kwit, M.; Esterhuysen, C.; Janiak, A. M.; Barbour, L. J. Dehydration of a crystal hydrate at subglacial temperatures. *Nature* **2023**, *616*, 288-292.
- (4) Martinez, C. R.; Iverson, B. L. Rethinking the term "pi-stacking". *Chem. Sci.* **2012**, *3*, 2191-2201.
- (5) Thakuria, R.; Nath, N. K.; Saha, B. K. The Nature and Applications of π – π Interactions: A Perspective. *Cryst. Growth Des.* **2019**, *19*, 523-528.
- (6) Shao, J.; Kuiper, B. P.; Thunnissen, A.-M. W. H.; Cool, R. H.; Zhou, L.; Huang, C.; Dijkstra, B. W.; Broos, J. The Role of Tryptophan in π Interactions in Proteins: An Experimental Approach. J. Am. Chem. Soc. 2022, 144, 13815-13822.
- (7) Yu, W.; Wang, X.-Y.; Li, J.; Li, Z.-T.; Yan, Y.-K.; Wang, W.; Pei, J. A photoconductive charge-transfer crystal with mixed-stacking donor–acceptor heterojunctions within the lattice. *Chem. Commun.* **2013**, *49*, 54-56.
- (8) Yu, P.; Zhen, Y.; Dong, H.; Hu, W. Crystal Engineering of Organic Optoelectronic Materials. *Chem.* **2019**, *5*, 2814-2853.

- (9) Chen, H.; Roy, I.; Myong, M. S.; Seale, J. S. W.; Cai, K.; Jiao, Y.; Liu, W.; Song, B.; Zhang, L.; Zhao, X.; et al. Triplet–Triplet Annihilation Upconversion in a Porphyrinic Molecular Container. *J. Am. Chem. Soc.* **2023**, *145*, 10061-10070.
- (10) Lee, S.; Chénard, E.; Gray, D. L.; Moore, J. S. Synthesis of Cycloparaphenyleneacetylene via Alkyne Metathesis: C70 Complexation and Copper-Free Triple Click Reaction. *J. Am. Chem. Soc.* **2016**, *138*, 13814-13817.
 - (11) Kitaigorodsky, A. I. Molecular Crystals and Molecules; Academic Press, 1973.
- (12) Saraswatula, V. G.; Saha, B. K. The effect of temperature on interhalogen interactions in a series of isostructural organic systems. *New J. Chem.* **2014**, *38*, 897-901.
- (13) Kumar, S.; Priyasha; Das, D. Molecular tiltation and supramolecular interactions induced uniaxial NTE and biaxial PTE in bis-imidazole-based co-crystals. *New J. Chem.* **2022**, *46*, 18465-18470.
- (14) Rather, S. A.; Saha, B. K. Understanding the elastic bending mechanism in a 9,10-anthraquinone crystal through thermal expansion study. *CrystEngComm* **2021**, *23*, 5768-5773.
- (15) Negi, L.; Kumar, S.; Dwivedi, B.; Das, D. Unusual Thermal Expansion in Hydrogen Bonded Network of an Organic Salt Induced by Large Transverse Vibration of Atoms. *Cryst. Growth Des.* **2021**, *21*, 1428-1433.
- (16) Saraswatula, V. G.; Bhattacharya, S.; Saha, B. K. Can the thermal expansion be controlled by varying the hydrogen bond dimensionality in polymorphs? *New J. Chem.* **2015**, *39*, 3345-3348.

- (17) Bhattacharya, S.; Saha, B. K. Interaction Dependence and Similarity in Thermal Expansion of a Dimorphic 1D Hydrogen-Bonded Organic Complex. *Cryst. Growth Des.* **2013**, 13, 3299-3302.
- (18) Bhattacharya, S. Interaction dependent anisotropic thermal expansion of a hydrogen bonded cocrystal. *J. Mol. Struct.* **2020**, *1220*, 128686.
- (19) Hutchins, K. M.; Unruh, D. K.; Verdu, F. A.; Groeneman, R. H. Molecular Pedal Motion Influences Thermal Expansion Properties within Isostructural Hydrogen-Bonded Co-crystals. *Cryst. Growth Des.* **2018**, *18*, 566-570.
- (20) Ding, X.; Unruh, D. K.; Groeneman, R. H.; Hutchins, K. M. Controlling thermal expansion within mixed cocrystals by tuning molecular motion capability. *Chem. Sci.* **2020**, *11*, 7701-7707.
- (21) Juneja, N.; Shapiro, N. M.; Unruh, D. K.; Bosch, E.; Groeneman, R. H.; Hutchins, K. M. Controlling Thermal Expansion in Supramolecular Halogen-Bonded Mixed Cocrystals through Synthetic Feed and Dynamic Motion. *Angew. Chem. Int. Ed.* **2022**, *61*, e202202708.
- (22) George, G. C., III; Unruh, D. K.; Groeneman, R. H.; Hutchins, K. M. Molecular Motion and Ligand Stacking Influence Thermal Expansion Behavior and Argentophilic Forces in Silver Coordination Complexes. *Cryst. Growth Des.* **2022**, *22*, 4538-4545.
- (23) Bosch, E.; Kruse, S. J.; Reinheimer, E. W.; Rath, N. P.; Groeneman, R. H. Regioselective [2 + 2] cycloaddition reaction within a pair of polymorphic co-crystals based upon halogen bonding interactions. *CrystEngComm* **2019**, *21*, 6671-6675.
 - (24) Harada, J.; Ogawa, K. Pedal motion in crystals. Chem. Soc. Rev. 2009, 38, 2244-2252.

- (25) Reddy, C. M.; Kirchner, M. T.; Gundakaram, R. C.; Padmanabhan, K. A.; Desiraju, G. R. Isostructurality, Polymorphism and Mechanical Properties of Some Hexahalogenated Benzenes: The Nature of Halogen···Halogen Interactions. *Chem. Eur. J.* **2006**, *12*, 2222-2234.
- (26) Hutchins, K. M.; Rupasinghe, T. P.; Ditzler, L. R.; Swenson, D. C.; Sander, J. R. G.; Baltrusaitis, J.; Tivanski, A. V.; MacGillivray, L. R. Nanocrystals of a Metal–Organic Complex Exhibit Remarkably High Conductivity that Increases in a Single-Crystal-to-Single-Crystal Transformation. *J. Am. Chem. Soc.* **2014**, *136*, 6778-6781.
- (27) Yu, X.; Guttenberger, N.; Fuchs, E.; Peters, M.; Weber, H.; Breinbauer, R. Diversity-Oriented Synthesis of a Library of Star-Shaped 2H-Imidazolines. *ACS Combinatorial Science* **2015**, *17*, 682-690.
- (28) Cliffe, M. J.; Goodwin, A. L. PASCal: a principal axis strain calculator for thermal expansion and compressibility determination. *J. Appl. Crystallogr.* **2012**, *45*, 1321-1329.
- (29) Macrae, C. F.; Sovago, I.; Cottrell, S. J.; Galek, P. T. A.; McCabe, P.; Pidcock, E.; Platings, M.; Shields, G. P.; Stevens, J. S.; Towler, M.; et al. Mercury 4.0: from visualization to analysis, design and prediction. *J. Appl. Crystallogr.* **2020**, *53*, 226-235.
- (30) Kalman, A.; Parkanyi, L.; Argay, G. Classification of the isostructurality of organic molecules in the crystalline state. *Acta Crystallogr., Sect. B: Struct. Sci., Cryst. Eng. Mater.* **1993**, *B49*, 1039-1049.
- (31) Bombicz, P.; May, N. V.; Fegyverneki, D.; Saranchimeg, A.; Bereczki, L. Methods for easy recognition of isostructurality lab jack-like crystal structures of halogenated 2-phenylbenzimidazoles. *CrystEngComm* **2020**, *22*, 7193-7203.

- (32) Saraswatula, V. G.; Sharada, D.; Saha, B. K. Stronger $\pi \cdots \pi$ Interaction Leads to a Smaller Thermal Expansion in Some Charge Transfer Complexes. *Cryst. Growth Des.* **2018**, *18*, 52-56.
- (33) Hunter, C. A.; Sanders, J. K. M. The nature of .pi.-.pi. interactions. *J. Am. Chem. Soc.* **1990**, *112*, 5525-5534.
- (34) Carter-Fenk, K.; Herbert, J. M. Electrostatics does not dictate the slip-stacked arrangement of aromatic π - π interactions. *Chem. Sci.* **2020**, *11*, 6758-6765.

For Table of Contents Only

Polymorphism and π Stacking Affect Thermal Expansion Behavior in Halogen-Bonded Cocrystals Based on 1,4-Diiodoperchlorobenzene

Gary C. George III, Mahshad Karimi, Navkiran Juneja, Daniel K. Unruh, Ryan H. Groeneman, and Kristin M. Hutchins

A pair of halogen-bonded, polymorphic cocrystals, along with an isostructural cocrystal was investigated. Although the halogen bonds are identical in all solids, the halogen-bond acceptor crystallized in either a face-to-face or edge-to-face stacked geometry. Differences in the π stacking between the polymorphs contributed to different coefficients and directions of thermal expansion in the solids.